Quantitative FWI characterization of reservoir properties at the CMC Newell County Facility

Qi Hu[1], *Matthew Eaid*[2], *Scott Keating*[3], *Kristopher Innanen*[1], *and Xiaohui Cai*[1]
[1] *Dept. of Geoscience, University of Calgary.* [2] *Chevron Technical Center, Houston.* [3] *ETH Zurich*

SUMMARY

We apply a sequential inversion scheme combining elastic FWI and Bayesian rock physics inversion to a VSP dataset acquired with accelerometers and collocated DAS fiber at the Carbon Management Canada's Newell County Facility. The goal is to build a baseline model of porosity and lithology parameters to support later monitoring of CO_2 storage. The key strategies include an effective source approach to cope with near-surface complications, a modeling strategy to simulate DAS data directly comparable to the field data, and a Gaussian mixture approach to capture the bimodality of rock properties. We perform FWI tests on the accelerometer, DAS, and combined accelerometer-DAS data. While the results can accurately reproduce either type of data, the elastic models from the accelerator data outperform the other two in matching well logs and identifying the target reservoir. We attribute this result to the insignificant advantage of DAS data, in this case, over accelerometer data, which also suffers from single-component measurements and lower signal-to-noise ratios. The porosity and lithology models predicted from the accelerometer elastic models are reasonably accurate at the well location and are geologically meaningful in spatial distribution.

INTRODUCTION

The Carbon Management Canada's (CMC) Newell County Facility is a platform for development and performance validation of technologies intended for measurement, monitoring and verification of CO_2 storage (Lawton et al., 2019; Macquet et al., 2022). In 2018, a vertical seismic profile (VSP) survey was acquired using accelerometers and collocated distributed acoustic sensing (DAS) fiber in an observation well at the field site (Hall et al., 2019). One of the goals of this survey was to obtain a baseline data set to compare against later monitoring data, gathered during the course of CO_2 storage.

A combination of seismic inversion for elastic properties and rock physics for predicting reservoir properties is a classical procedure in reservoir characterization (Doyen, 2007; Grana et al., 2021). The seismic inversion is generally performed using AVO (amplitude-versus-offset). This approach is simple to implement and computationally fast. FWI methods have the capacity to produce a more accurate elastic model by involving a more complete subset of data information (Tarantola, 1986; Mallick and Adhikari, 2015; Hu et al., 2021), therefore appear to be a potentially powerful tool for reservoir characterization. In CO_2 applications, progress has been reported in combining FWI and rock physics for predicting CO_2 saturation (Queißer and Singh, 2013; Dupuy et al., 2021; Hu et al., 2023). In these studies, the recovered baseline model of reservoir properties, such as porosity and lithology, help reduce the uncertainty in fluid monitoring.

At the Newell County Facility, one of the challenges FWI faces is the near-surface heterogeneity. The unconsolidated nature of the sediment in proximity to Earth's surface leads to complex seismic wave propagation that is heavily influenced by surface waves, attenuation and dispersion, and spatially varying source signatures. In the absence of robust near-surface information, Keating et al. (2021) proposed an effective source approach for VSP FWI. The idea is to remove the near surface from inversion by introducing an unknown a variable characterizing the wavefield at depth. Another challenge for FWI is the incomplete nature of the data we record. The advent of DAS supplies an additional subset of the data that could contain the information required to propel FWI forward (Eaid et al., 2020; Pan et al., 2023). In fact, the conventional 3C geophones directly measure multiple wavefield components, and do so with a relatively high signal-to-noise ratio (SNR), but are limited in the low-frequencies they can sense and where they can be cost-effectively deployed; DAS senses low-frequencies effectively, and can occupy boreholes without disturbing production processes, but have a generally lower SNR and are fundamentally single-component. The two sensor types can be viewed as supplying complementary datasets.

Our goal is to explore the potential of FWI in quantitative seismic reservoir characterization. First, we present the FWI and rock physics inversion methods. We then give a brief introduction to the VSP experiment at the CMC Newell County Facility. Finally, we apply a sequential inversion scheme combing FWI and rock physics to the processed data, including both accelerometer and DAS measurements.

METHODS

Simultaneous FWI for wavefield and elastic model

The FWI problem can be framed as an attempt to minimize the mismatch between data and model predictions, subject to a wave propagation model:

$$\min_{\mathbf{m}} E = \frac{1}{2}\|\mathbf{Ru}-\mathbf{d}\|_2^2 \quad \text{subject to} \quad \mathbf{A}(\mathbf{m})\mathbf{u} = \mathbf{f}, \tag{1}$$

where E is the objective function, $\mathbf{d}$ is the observed data, $\mathbf{R}$ is a sampling matrix representing receiver measurement. Here we consider the a 2D frequency-domain isotropic-elastic wave equation (Pratt, 1990): $\mathbf{A}$ is impedance matrix, $\mathbf{u}$ is the displacement wavefield, and $\mathbf{f}$ is the source term.

The Lagrangian of the minimization problem is

$$L(\mathbf{m},\mathbf{u},\lambda) = \frac{1}{2}\|\mathbf{Ru}-\mathbf{d}\|_2^2 + \Re\langle \mathbf{Au}-\mathbf{f}, \lambda\rangle, \tag{2}$$

where λ is the Lagrange multiplier, $\Re$ indicates the real part, and $\langle .,. \rangle$ is the scalar product. Let $\bar{\mathbf{u}}$ denotes the solution of the wave equation, such that $\mathbf{A}\overline{\mathbf{u}} = \mathbf{f}$, we have $L(\mathbf{m}, \overline{\mathbf{u}}, \lambda) = E$, and the gradient yields

$$\nabla_{\mathbf{m}} E = \frac{dL(\mathbf{m}, \overline{\mathbf{u}}, \lambda)}{d\mathbf{m}} = \frac{\partial L(\mathbf{m}, \overline{\mathbf{u}}, \lambda)}{\partial \mathbf{m}} + \frac{\partial L(\mathbf{m}, \overline{\mathbf{u}}, \lambda)}{\partial \mathbf{u}} \frac{\partial \overline{\mathbf{u}}}{\partial \mathbf{m}}. \quad (3)$$

The adjoint state $\overline{\lambda}$ is defined by $\frac{\partial L(\mathbf{m}, \overline{\mathbf{u}}, \overline{\lambda})}{\partial \mathbf{u}} = 0$, which is equivalent to

$$\mathbf{A}^{\dagger} \overline{\lambda} = \mathbf{R}^{\dagger} (\mathbf{d} - \mathbf{R} \overline{\mathbf{u}}), \quad (4)$$

where † represents conjugate transpose. Eq. (3) is reduced to

$$\nabla_{\mathbf{m}} E = \frac{\partial L(\mathbf{m}, \overline{\mathbf{u}}, \overline{\lambda})}{\partial \mathbf{m}}. \quad (5)$$

It then follows from eq. (2) that the individual components of the gradient vector can be expressed as

$$\nabla_{m_i} E = \Re \langle \frac{\partial \mathbf{A}}{\partial m_i} \overline{\mathbf{u}} \, , \overline{\lambda} \, \rangle. \quad (6)$$

We consider here an effective source approach, which attempts to remove near surface from the inversion. We imagine a line source $\mathbf{f}^*$ at depth z^* such that, when activated, it reproduces the wavefield that would be obtained by propagation through the near surface. The optimization problem is given by

$$\min_{\mathbf{m}^*, \mathbf{f}^*} E = \frac{1}{2} \|\mathbf{R}^* \mathbf{u}^* - \mathbf{d}^*\|_2^2 \quad \text{subject to} \quad \mathbf{A}^*(\mathbf{m}^*) \mathbf{u}^* = \mathbf{f}^*, \quad (7)$$

where each * variable is only allowed to take values below z^*. Eq. (7) is effectively the same optimization problem as eq. (1), with the exception that we define the problem on a smaller model domain, and invert for both an unknown model $\mathbf{m}^*$ and an unknown source $\mathbf{f}^*$. We can obtain the gradient with respect to $\mathbf{f}^*$ in a way similar to the model gradient. The result is

$$\nabla_{f_i} E = -\overline{\lambda}_i, \quad (8)$$

where λ_i is the adjoint wavefield at an effective source location indexed by i. In practice, we initialize $\mathbf{f}^*$ using the modeled wavefield at depth z^* from the initial model.

FWI incorporating DAS data

DAS fiber response is proportional to the strain induced in the fiber by seismic wavefield. Following the approach of Eaid et al. (2020), we can generate strain data directly in forward modeling to compare with the field DAS data. For straight fibers deployed in vertical wells, the fibers have a single, vertical tangent direction, resulting in a DAS system sensitive only to the vertical normal strain. We compute the tangential stain e_{tt} on a grid staggered to that of the displacements, so the strain at a cell is approximated as a weighted sum of the neighboring displacements u_z. The receiver matrix $\mathbf{R}$ can be understood more generally as an operator that transforms the simulated wavefield into quantities directly comparable to the observed data. Therefore, we can include DAS data in FWI by simply reformulating R. We design some rows of $\mathbf{R}$ to map the displacement to the accelerometer positions and the others to compute the tangential strain at channel positions along the fiber. The modeling process, $\mathbf{d} = \mathbf{R}\mathbf{u}$, can be expressed as

$$\begin{bmatrix} d_x^1 \\ \vdots \\ d_x^{N_a} \\ d_z^1 \\ \vdots \\ d_z^{N_a} \\ e_{tt}^1 \\ \vdots \\ e_{tt}^{N_d} \end{bmatrix} = \begin{bmatrix} & 1 & & & & & & \\ \vdots & & & & & & & \\ & & & & & 1 & & \\ & & 1 & & & & & \\ \vdots & & & & & & & \\ & & & & & & 1 & \\ & w_1 & w_2 & \dots & w_3 & w_4 & & \\ \vdots & & & & & & & \\ & & & w_1 & w_2 & \dots & w_3 & w_4 \end{bmatrix} \begin{bmatrix} u_x^1 \\ u_z^1 \\ u_x^2 \\ u_z^2 \\ \vdots \\ u_x^N \\ u_z^N \end{bmatrix}, \quad (9)$$

where N is the total number of grid cells, N_a and N_d are the numbers of accelerometer and DAS sensors, and w_1, w_2, w_3, w_4 are finite-difference coefficients. This formulation also allows us to include a weighting matrix in the objective function to control the relative importance of accelerometer and DAS data.

Bayesian rock physics inversion

Once we have obtained a model of elastic properties $\mathbf{m}$ from seismic data, we then aim to estimate the rock properties $\mathbf{r}$, from $\mathbf{m}$ as the solution of another inverse problem

$$\mathbf{m} = g(\mathbf{r}) + \varepsilon, \quad (10)$$

where g is the rock physics model and ε is the data error. In this study, the vector $\mathbf{m}$ includes P- and S-wave velocities plus density, and the model variable $\mathbf{r}$ includes porosity and mineral volume fractions. We operate in a Bayesian setting to assess the the conditional probability $P(\mathbf{r}|\mathbf{m})$:

$$P(\mathbf{r}|\mathbf{m}) = \frac{P(\mathbf{r}, \mathbf{m})}{P(\mathbf{m})} = \frac{P(\mathbf{m}|\mathbf{r}) P(\mathbf{r})}{P(\mathbf{m})}, \quad (11)$$

where $P(\mathbf{r}, \mathbf{m})$ is the joint distribution of rock and elastic properties, $P(\mathbf{r})$ is the prior distribution, $P(\mathbf{m}|\mathbf{r})$ is the likelihood function, and $P(\mathbf{m})$ is a normalizing constant.

We use the semi-analytical approach of Grana and Rossa (2010) to estimate the conditional probability $P(\mathbf{r}|\mathbf{m})$. First, we generate a set of Monte Carlo samples from the prior distribution $P(\mathbf{r})$ and apply rock physics modeling to obtain the corresponding set of elastic properties; we then use these samples as a training dataset to estimate the joint distribution $P(\mathbf{r}, \mathbf{m})$. As a consequence, the conditional distribution $P(\mathbf{r}|\mathbf{m})$ is again a Gaussian mixture with analytical expressions.

APPLICATIONS

VSP experiment at CMC Newell County Facility

The field site houses three wells, including the well being used for CO_2 injection, and two observation wells, colloquially referred to as the geophysics and geochemistry wells. The injection of CO_2 at a shallow depth of 300 m is designed to simulate leakage of CO_2 from a deep sequestration site. We focus on the multi-azimuth walk-away VSP dataset acquired in September 2018 (Fig. 1). For this survey, a string of Inova 3C VectorSeis

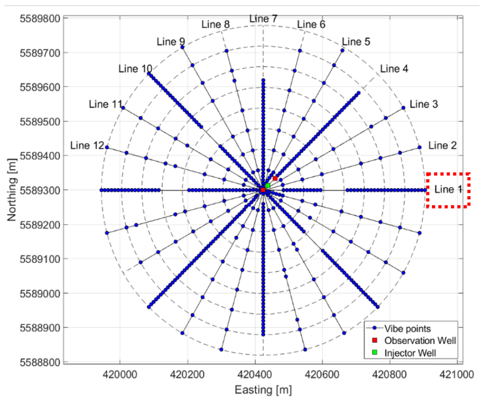

Figure 1: Shot geometry of the multi-azimuth walk-away VSP experiment at the Newell County Facility. The two red squares mark the locations of the geophysics and geochemistry wells, offset from the injection well by 20 m to south-west and 30 m to north-east, respectively.

.

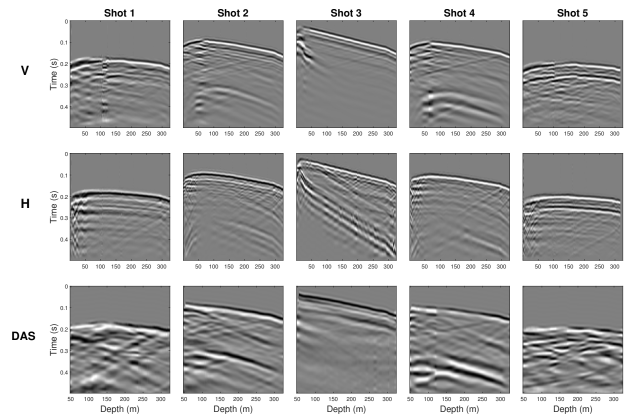

Figure 2: Processed accelerometer and DAS data. Rows top to bottom: vertical component of acceleration, horizontal component of acceleration, and DAS-recorded strain. Each column represents the data of a single shot.

accelerometers were deployed at 1 m spacing from surface to the bottom hole at about 324 m depth. In addition, the geophysics well houses a straight DAS fiber over the entire length of the well, which is part of a 5 km DAS fiber loop permanently buried in the field. We consider 2D FWI, and restrict our analysis to the data generated by source line 1.

The seismic data have been carefully processed to be more comparable to simulated data generated by modeling procedures (Eaid et al., 2022). Fig. 2 plots the processed accelerometer and DAS data for five shot points, which represent a portion of the input data for FWI. The result is a high-fidelity two-component accelerometer dataset, whereas the DAS dataset has a relatively low signal-to-noise ratio, especially at far-offset.

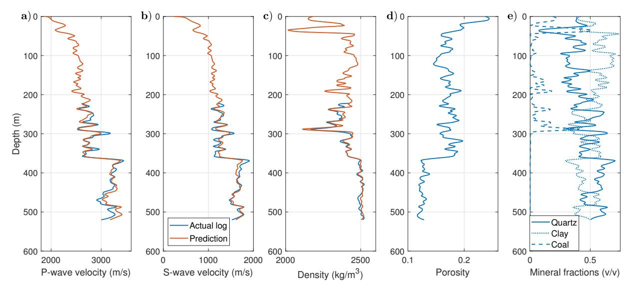

Figure 3: Well logs (upscaled) of the injection well: (a) P-wave velocity, (b) S-wave velocity, (c) density, (d) total porosity, and (e) the volume fractions of quartz, clay, and coal. Well log data are in blue and rock physics model predictions in orange.

Rock physics analysis of well-log data

The injection zone is at a depth of approximately 300 m below ground surface, and it is a 7-m-thick, fine to medium-grained sandstone. The overlying sealing succession is composed of interbedded mudstone, fine-grained sandstone, and uncleated coals that directly overlies the injection zone. Based on the well log data of the range 223-520 m, we have constructed a rock physics model based on the soft-sand model and Gassmann's equations:

$$(V_\mathrm{P}, V_\mathrm{S}, \rho) = g(\phi, V_\mathrm{qu}, V_\mathrm{cl}, V_\mathrm{co}), \tag{12}$$

where V_qu, V_cl, and V_co represent the volume fractions of quartz, clay, and coal, respectively, and $V_\mathrm{qu} + V_\mathrm{cl} + V_\mathrm{co} = 1$. Because the in-stu hydrocarbon saturation is sufficiently small, the water saturation was assumed to be 100%. Given its visible fit to the data, the model was then used to reconstruct the velocity and density logs missed at shallow depths 0-223 m. The predictions have a good match with the first-arrival traveltimes picked on zero-offset data (Kolkman-Quinn, 2022).

Elastic FWI results

The model we consider is 1000 m wide by 350 m deep, with

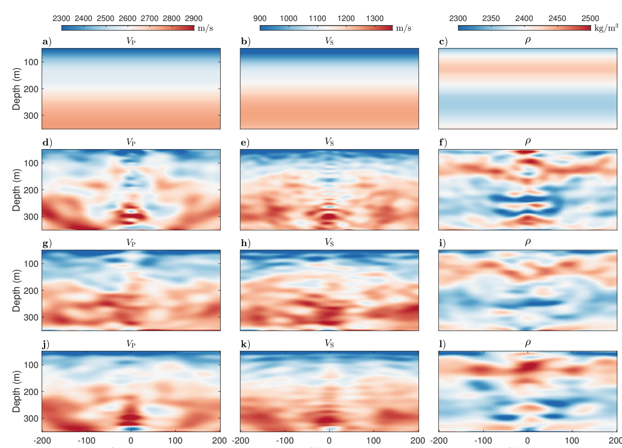

Figure 4: (a-c) Initial models and inverted models from (d-f) accelerometer, (g-i) DAS, and (j-l) combined accelerometer-DAS data.

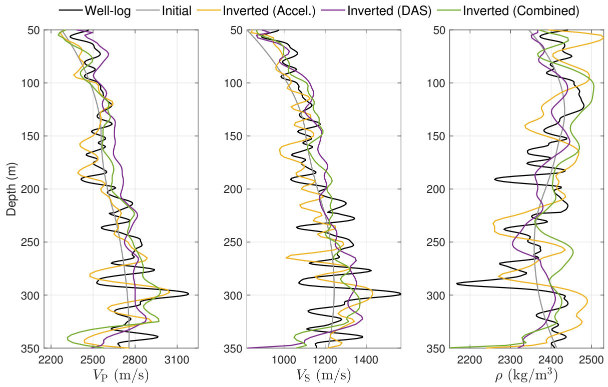

Figure 5: Comparison of the well logs and model profiles.

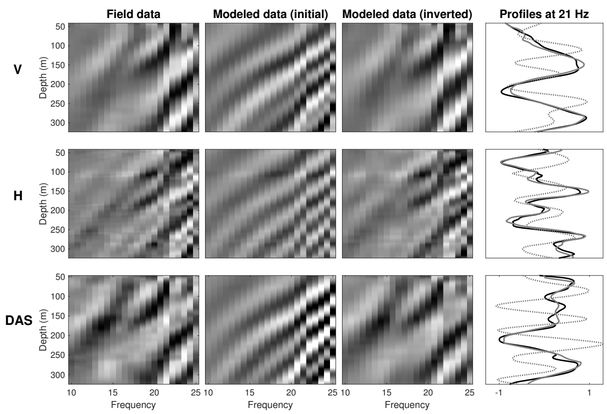

Figure 6: Real part of frequency domain data

2.5 m grid spacing. We use 63 shots. The minimum frequency we use is 10 Hz and the maximum frequency is 25 Hz. The initial models are created by smoothing the well logs. Due to limited aperture, we only demonstrate the recovered models within 200 m offset. The results are summarized in Fig. 4. The inverted models from either dataset exhibit sufficient updates from initial one but have different features. Observation of the model profiles (Fig. 5) suggest that the accelerometer models correlate strongly to well logs and capture the large contrast between the caprock and target reservoir (300 m). The DAS models fail to identify the reservoir, and this brings a great obstacle for us to use the DAS data alone to predict reservoir parameters. In Fig. 6, the normalized frequency-domain measured and modeled data for the shot at 70 m offset are plotted. As this comparison demonstrates, the data misfit is significantly reduced after inversion. In fact, across all shots, data misfit was reduced by 95% for the accelerometer data and 70% for the DAS data.

Rock physics inversion results

In this section, we adopt the FWI models from the accelerometer data to predict the spatial distribution of reservoir properties. In Fig. 7, the MAP models are plotted. We can find several positive features from this result, the most important of

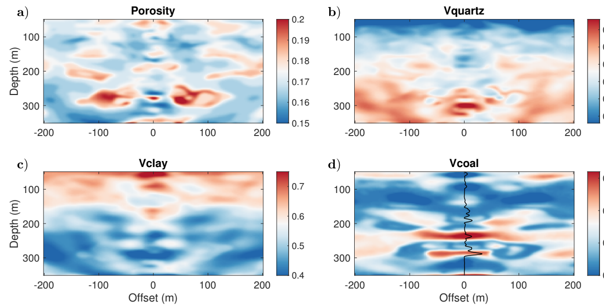

Figure 7: Inverted models of (a) porosity, (b) quartz volume, (c) clay volume, and (d) coal volume (superimposed the actual log).

which is the successful identification of the laterally continuous coal zones in the depth range of 200 m to 300 m. These coal zones are estimated to be the main sealing units above the injection area. Also, the inverted clay volume is relatively high throughout the model space, which is consistent with the geological background. The inverted porosity values are relatively stable, however, the model exhibits a strong degree of blockiness and may contain some artifacts.

CONCLUSIONS

In this study, we focus on integrating FWI and rock physics to recover porosity and lithology models from the measured data. The inverted elastic models from the accelerometer, DAS, and combined accelerometer-DAS data exhibited different features. In the absence of other verification methods, we judged that the result with the acceleration data alone is most accurate according to the degree of matching with well-log data. We therefore used this result for the subsequent inversion of reservoir parameters and obtained meaningful predictions. This study represents an attempt to bring FWI technology into practical use for reservoir characterization.

ACKNOWLEDGMENTS

This work was funded by CREWES industrial sponsors and NSERC (Natural Science and Engineering Research Council of Canada) through the grant CRDPJ 543578-19. The data were acquired through a collaboration with the Containment and Monitoring Institute, Carbon Management Canada.

REFERENCES

Buland, A., and H. Omre, 2003, Bayesian linearized AVO inversion: Geophysics, **68**, 185–198.

Doyen, P., 2007, Seismic reservoir characterization: An earth modelling perspective: EAGE publications.

Dupuy, B., A. Romdhane, P. Eliasson, and H. Yan, 2021, Combined geophysical and rock physics workflow for quantitative CO_2 monitoring: International Journal of Greenhouse Gas Control, **106**, 103217.

Eaid, M., S. Keating, and K. Innanen, 2022, Combined elastic fwi of accelerometer and das vsp data from a co2 sequestration test site in newell county, alberta: SEG International Exposition and Annual Meeting, SEG, D011S045R003.

Eaid, M. V., S. D. Keating, and K. A. Innanen, 2020, Multiparameter seismic elastic full-waveform inversion with combined geophone and shaped fiber-optic cable data: Geophysics, **85**, R537–R552.

Grana, D., T. Mukerji, and P. Doyen, 2021, Seismic reservoir modeling: Theory, examples, and algorithms: John Wiley & Sons.

Grana, D., and E. D. Rossa, 2010, Probabilistic petrophysical-properties estimation integrating statistical rock physics with seismic inversion: Geophysics, **75**, O21–O37.

Hall, K. W., K. L. Bertram, M. Bertram, K. Innanen, and D. C. Lawton, 2019, Simultaneous accelerometer and optical fibre multi-azimuth walk-away vsp experiment: Newell county, alberta, canada: Presented at the SEG International Exposition and Annual Meeting, OnePetro.

Hu, Q., D. Grana, and K. A. Innanen, 2023, Feasibility of seismic time-lapse monitoring of co2 with rock physics parametrized full waveform inversion: Geophysical Journal International, **233**, 402–419.

Hu, Q., S. Keating, K. A. Innanen, and H. Chen, 2021, Direct updating of rock-physics properties using elastic full-waveform inversion: Geophysics, **86**, MR117–MR132.

Keating, S., M. Eaid, and K. Innanen, 2021, Effective sources: removing the near surface from the vsp fwi problem: CREWES Research Reports, **33**.

Keating, S., and K. A. Innanen, 2019, Parameter cross-talk and leakage between spatially-separated unknowns in viscoelastic FWI: 89th Annual International Meeting, SEG, Expanded Abstracts, 1415–1419.

Kolkman-Quinn, B. J., 2022, Time-lapse vsp monitoring of co2 sequestration at the cami field research station: Master's thesis, Science.

Lawton, D. C., J. Dongas, K. Osadetz, A. Saeedfar, and M. Macquet, 2019, Development and analysis of a geostatic model for shallow CO_2 injection at the field research station, southern alberta, canada: Geophysics and Geosequestration. Cambridge University Press, Cambridge, **280**, 296.

Macquet, M., D. Lawton, K. Osadetz, G. Maidment, M. Bertram, K. Hall, B. Kolkman-Quinn, J. M. Parra, F. Race, G. Savard, et al., 2022, Overview of carbon management canada's pilot-scale co2 injection site for developing and testing monitoring technologies for carbon capture and storage, and methane detection: CSEG Recorder, **47**, 1–27.

Macquet, M., D. C. Lawton, A. Saeedfar, and K. G. Osadetz, 2019, A feasibility study for detection thresholds of CO_2 at shallow depths at the cami field research station, newell county, alberta, canada: Petroleum Geoscience, **25**, 509–518.

Mallick, S., and S. Adhikari, 2015, Amplitude-variation-with-offset and prestack-waveform inversion: A direct comparison using a real data example from the Rock Springs Uplift, Wyoming, USA: Geophysics, **80**, B45–B59.

Mavko, G., T. Mukerji, and J. Dvorkin, 2020, The rock physics handbook: Cambridge university press.

Métivier, L., R. Brossier, S. Operto, and J. Virieux, 2017, Full waveform inversion and the truncated Newton method: SIAM Review, **59**, 153–195.

Pan, W., L. Qu, K. A. Innanen, J. Dettmer, M. Macquet, D. Lawton, and Y. Wang, 2023, Imaging near-surface s-wave velocity and attenuation models by full-waveform inversion with distributed acoustic sensing-recorded surface waves: Geophysics, **88**, R65–R78.

Pratt, R. G., 1990, Frequency-domain elastic wave modeling by finite differences: A tool for crosshole seismic imaging: Geophysics, **55**, 626–632.

Queißer, M., and S. C. Singh, 2013, Full waveform inversion in the time lapse mode applied to CO_2 storage at Sleipner: Geophysical prospecting, **61**, 537–555.

Tarantola, A., 1986, A strategy for nonlinear elastic inversion of seismic reflection data: Geophysics, **51**, 1893–1903.